Automatic Segmentation of the Vessel Lumen from 3D CTA Images of Aortic Dissection

Tamás Kovács[1], Philippe Cattin[1], Hatem Alkadhi[2], Simon Wildermuth[3] and Gábor Székely[1]

[1]Computer Vision Group, ETH Zürich, 8092 Zürich, Switzerland
[2]Institute of Diagnostic Radiology, University Hospital, 8092 Zürich,
[3]Institut fuer Radiologie, Kantonsspital St. Gallen, 9000 St. Gallen, Switzerland
Email: [1]{kovacs, cattin, szekely}@vision.ee.ethz.ch,
[2]hatem.alkadhi@usz.ch, [3]simon.wildermuth@kssg.ch

Abstract. Acute aortic dissection is a life-threatening condition and must be diagnosed and treated promptly. For treatment planning the reliable identification of the true and false lumen is crucial. However, a fully automatic Computer Aided Diagnosing system capable to display the different lumens in an easily comprehensible and timely manner is still not available.
In this paper we present the first step towards such a system, namely a method that segments the entire aorta without any user interaction. The method is robust against inhomogeneous distribution of the contrast agent generally seen in dissected aortas, high-density artifacts, and the dissection membrane separating the true and the false lumen.

1 Introduction

Acute aortic dissection is a life-threatening condition and must be diagnosed and treated promptly. The reliable identification of the true and false lumen is crucial for treatment planning. This is, however, a difficult task, even for trained professionals. A fully automatic Computer Aided Diagnosing (CAD) system capable to display the different lumens in an easily comprehensible way is still not available. It is thus the aim of this research to provide the radiologists generic tools to support diagnosis and treatment planning. In order to accomplish such a CAD system, an accurate segmentation of the entire aorta including the aortic arch as well as the ascending and descending segments is essential.

Different solutions for the aorta segmentation can be found in literature. These include vessel axis extraction and border estimation [1, 2], neural network [3], watershed-based [4], region growing [5] and level set-based [6] approaches. All of these methods segment just a well defined part of the aorta, require manual initialization and some even user intervention. Moreover, these methods are not robust against the disturbing artifacts in the image data like the different densities of the contrast agent caused by flow variations in the two lumens, reconstruction errors due to high contrast agent density [7] and last but not least they are not able to deal with the dissection membrane within the aortic lumen.

We have developed a method for the fully automatic segmentation of the aorta based on the Hough transformation (HT) and a deformable model (DM) framework. An extensive survey of the DMs is given in [8]. The DMs always require an accurate initialization of the object. Behrens in [9] suggests a Hough-based algorithm combined with a Kalman filter to obtain an approximate segmentation of tubular structures. The drawback of this approach is, however, the need for three initial parameters (starting point of the aorta, the aorta radius, and an approximate axis direction). Additionally, the large number of applied HTs make the segmentation relatively slow. In comparison to this approach, our method incorporates more a priori anatomical knowledge about the shape of the aortic arch and therefore needs no initial parameters.

2 Description of the method

We present a robust, model based approach capable to segment the aorta regardless the inherent deficiencies present in CTA images of aortic dissections. The method is based on the observation that on the one hand the aorta lumen has an approximately circular cross section and on the other hand the aortic arch forms a 180°-sector of a torus. Using this a priori knowledge as a simple model in combination with the Hough transformation yields a reliable aorta segmentation method. As will be shown in the results, the circular shape of the aorta is an ideal constraining factor to support the segmentation process.

In order to create an initial mesh for the DM, two seed points must be determined in the ascending as well as in the descending aorta. The points can be placed by a user (semiautomatic segmentation) or they can be calculated automatically as will be described next.

In the first step the region of the heart is detected by calculating the average intensity of all axial slices. As the heart chambers have large cross sections filled with contrast agent, the highest average intensity is a reliable locator. Starting from the slice with the highest average intensity 20 axial slices were taken with a distance of 1 cm. On each of these slices the two circles defined by the strongest Hough-peaks were detected which mostly corresponded to the ascending and descending aorta. For the first slices, still in the heart region, no such circles are detected. In the next step, the centers of the detected circles from all of the slices are projected to an axial plane, which results in a set of points given by (x, y) coordinates. In order to obtain the positions of the aorta the set of points have to be spatially clustered, which in our case was performed with the K-means algorithm. According to our experiments the HT within the given interval superior the heart can detect not only the ascending and descending aorta but also the spine (although with a lower probability). Based on this consideration we have set the number of clusters to three. The centers of the two largest clusters in terms of number of elements approximate the position of the ascending and descending aorta. As the last step we search for the slice closest to the heart on which the two detected circles are members of the respective

clusters. The centers of these two circles serve as the seed points (C_A, C_D) of the ascending and descending aorta, see Fig. 2(a)/1.

Based on the relative position of (C_A, C_D) the radius r of the aortic arch can be estimated with $r = |C_A - C_D|/2$, see Fig. 2(a)/2. With an additional HT on the reformatted slice perpendicular to the connecting line of the circle centers C_A and C_D, the superior point of the aortic arch can be estimated as shown in Fig. 2(a)/3. Since the aorta and the pulmonary artery are located close to each other, in fact two different circles are detected in the preceding step. From anatomical knowledge, however, we know that the aorta lies superior to the pulmonary artery (Fig. 2(a)/4) yielding $C_{90°}$ as the circle center. The center C_{arch} of the aortic arch, Fig. 2(b), can now be determined with $C_{arch} = C_{90°} + r(\overrightarrow{C}_{AD} - \overrightarrow{C}_{90°})/(|\overrightarrow{C}_{AD} - \overrightarrow{C}_{90°}|)$ were $\overrightarrow{C}_{AD} = \overrightarrow{C}_A + (\overrightarrow{C}_D - \overrightarrow{C}_A)/2$. So far the aorta centerline is defined by the three circle centers C_A, $C_{90°}$, and C_D. For further refinement, additional slices are reformatted in 15 degree steps by pivoting around C_{arch}, yielding 13 additional circle centers and aorta diameter pairs (C_i, d_i) $\forall\ i = 0°, 15°, ..., 180°$, see Fig. 2(b)/5. To avoid outliers in the first place, the two connecting lines between $(C_{0°}, C_{90°})$ and $(C_{90°}, C_{180°})$ are taken as a rough aortic arch model and the ROI in every reformatted slice can be restricted to 2.5-times the average aorta diameter. Defining tight ROIs not only increases the robustness, but also reduces the computational load of the approach, as the time consuming HTs are only applied to small subimages found by the model assumptions with the previously estimated parameters. Based on the center points C_i, a good approximation for the midline of the aortic arch is given. Starting from $C_{180°}$ the aorta segmentation is extended, in 2 cm steps, through the descending aorta towards the iliac bifurcation Fig. 2(b)/6. For computational efficiency the ROI is located at the same position as in the last slice and the ROI is limited to 70×70 mm^2. As the vessel's cross section close to the bifurcation loses its circular shape, the distal end of the descending aorta can be easily detected and the process stopped. The centerline of the aorta and the arch is then interpolated from the center points using a cubic spline, see Fig. 2(b)/7.

To further refine the segmentation, an elastically deformable model (DM) is used. The initial mesh of the DM can be easily generated using the aorta centerline with the associated aorta diameters. This initialization is then optimized using the mass-spring analogy as described in [10].

3 Results

The method was applied to 21 patients of which 3 had normal healthy anatomy and 8 abdominal aortic dissection. The 10 remaining patients have shown multiple pathologies as 3 aneurisms, 6 stenosis, and 8 stent grafts. The CT datasets typically consisted of $500 - 650$ slices of 512×512 pixels using 16-bit quantization, with a pixel size of $0.6 - 0.65$ mm, and an effective slice thickness of 2 mm.

From the 21 datasets only the 3 aneurism and one heavy stenosis case failed, as our current implementation can not yet handle the variing lumen diameter. In spite of the sometimes bad signal-to-noise ratio and the presence of distractor

Fig. 1. (a) The detection of the three initial circles to estimate the parameters of the aortic arch (b) the refinement of the aortic arch and the descending aorta with additional circles. The steps described in the text are highlighted with numbers

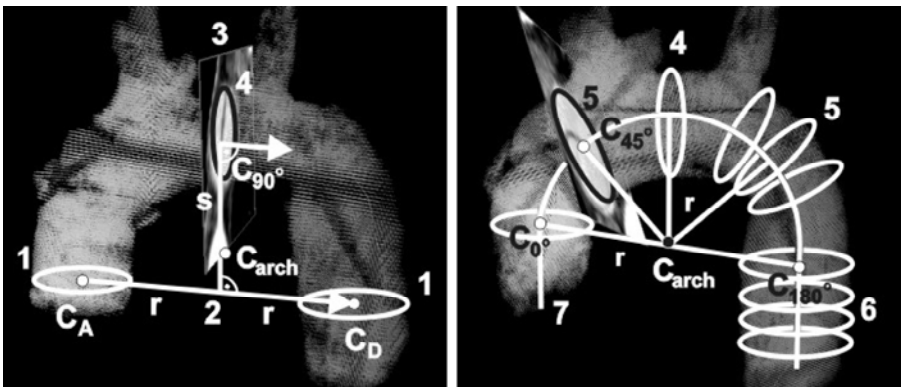

(a) (b)

objects like stents, the segmentation process was successful in all other cases, as demonstrated on some examples in Fig. 2.

To obtain a quantitative assessment, the datasets were manually segmented. The mesh of these segmentations were taken as the ground truth and compared to the results of the 17 successful segmentations. To quantify the performance, we determined the average distance of the two meshes perpendicular to the manual segmentation. Our method performed equally well for the group of healthy patients (3), dissections (8), small stenosis (2) resulting in an overall average error of 1.1 ± 0.17 mm. The best segmentation had an average distance of 0.84 ± 0.92 mm and the worst one of 1.33 ± 1.04 mm. The results were less satisfactory for the stent graft cases with an average distance of 2.22 ± 0.33 mm.

The average time required to perform a manual segmentation was 40 min per dataset. In contrast, the processing time was less than 1 min for the semiautomatic segmentation (the two initial points were placed by a user), and about 6 min for the fully automatic procedure using a standard 2.4 GHz PC.

4 Discussion and conclusion

In this paper we presented an automatic method for the segmentation of the aorta using a model based approach. The method uses HTs to detect the approximately circular shape of the aorta on the individual slices orthogonal to the vessel, and a 3D elastically deformable mass-spring model to more accurately adjust the detected contour to the aortic lumen. The method is robust against acquisition artifacts typically present in 3D CTA images of aortic dissections.

The performance of the method has been evaluated on CT angiographic images of 21 patients. The results have been satisfactory, even if manual segmentation by a human expert would have produced a more accurate delineation of the lumen on some slices.

Fig. 2. (a) Accurate segmentation of the aortic arch displayed on an axial slice, (b) segmentation with the dissection membrane close the lumen wall, (c) the aorta outline on a slice of a noisy dataset, (d) 3D rendering of the segmented aorta

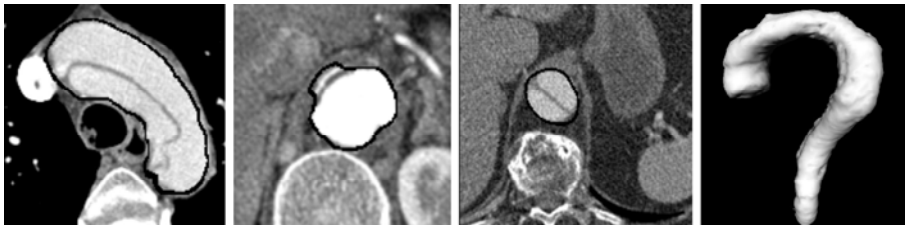

(a) (b) (c) (d)

Our future work will concentrate on the detection of the dissection membrane within the identified region of interest. The detected membrane is then used to identify and visualize the true and false lumen of the aorta.

Acknowledgments. This work has been supported by the CO-ME/NCCR research network of the Swiss National Science Foundation (`http://co-me.ch`).

References

1. Verdonck B, Bloch I, Maître H, et al. Accurate Segmentation of Blood Vessels from 3D Medical Images. In: IEEE Int Conf on Image Process; 1996. p. 311–314.
2. Wink O, Niessen WJ, Viergever MA. Fast Delineation and Visualization of Vessels in 3-D Angiographic Images. IEEE Trans Med Imaging 2000;19(4):337–346.
3. Katz WT, Merickel MB. Aorta Detection In Magnetic Resonance Images Using Multiple Artificial Neural Networks. In: Annual Int Conf of the IEEE Eng Med Biol Mag; 1990. p. 1302–1303.
4. Tek H, Akova F, Ayvaci A. Region competition via local watershed operators. In: IEEE Comput Soc Conf on Comput Vis and Pattern Recog; 2005. p. 361–368.
5. Pohle R, Toennies KD. Segmentation of Medical Images Using Adaptive Region Growing. In: SPIE Med Imaging Conf. vol. 4322; 2001.
6. Loncarić S, Subasić M, Soratin E. 3-D deformable model for abdominal aortic aneurysm segmentation from CT images. First Int Workshop on Image and Signal Process and Anal 2000.
7. Baissalov R, Sandison GA, Donnelly BJ, et al. Suppression of high-density artefacts in x-ray CT images using temporal digital subtraction with application to cryotherapy. Phys Med Biol 2000;45:53–59.
8. McInerney T, Terzopoulos D. Deformable Models in Medical Image Analysis: A Survey. Med Image Anal 1996;1:91–108.
9. Behrens T, Rohr K, Stiehl HS. Robust Segmentation of Tubular Structures in 3-D Medical Images by Parametric Object Detection and Traking. IEEE Trans Syst Man Cybern B 2003;33:554–561.
10. Zsemlye Gabriel. Shape Prediction from Partial Information. Ph.D. thesis. Computer Vision Laboratory, ETH Zurich, Switzerland; 2005.